

Generalized Periodic Disturbance Observer Technology with Automatic Learning Functions

Yugo Tadano,
Kazunobu Oi,
Takashi Yamaguchi

Keywords Harmonics suppression, Active filter, Torque ripple suppression control, PM motor, Auto-tuning

Abstract

Periodic disturbance, which occurs intermittently at a specific frequency, gives rise to various problems such as vibration, noise, and resonance. For solutions, the industry engages in the R&D activities like suppression and control technologies to eliminate periodic disturbance. Simultaneously, however, there are challenges regarding control instability and performance deterioration due to complicated variations in system characteristics. In addition, there is pressing demand in the markets for auto-tuning technologies that are expected to save man-hours for control adjustments.

Our newly developed generalized periodic disturbance observer method comes in a simple control configuration, with a learning function. Even for a system that has unknown characteristics or is expected to cause variations, this method offers features to perform automatic stabilization of suppression control and ensure prevention of performance deterioration. This paper explains the basic theory and demonstrates the usefulness of the proposed method by applying it to power active filters and PM motor torque ripple suppression.

1 Preface

When designing a control system for large-scale and complicated electrical and mechanical facilities, various factors in the control system such as characteristic changes, load variations, resonance, disturbance, and non-linearity can be a cause of deterioration in system controllability. In a worst case scenario, the system becomes unstable and control failure may occur. It is necessary to establish a robust control system for protection against these causes accordingly. In particular, periodic disturbance, which is caused intermittently at a specific frequency, appears frequently in the result of control and it can give rise to serious problems such as expansion of resonance phenomena.

For example, a periodic disturbance like harmonics in the power distribution system can adversely affect the power distribution equipment in the system. This type of disturbance is therefore controlled and stipulated according to the guideline in regard to harmonics. Going forward, the introduction of smart grids and distributed power systems by renewable energy resources will be promoted. When an unspecified large number of such power

converters are interconnected with utility power grids, the sources of harmonics are complicated. In addition, there will be fluctuations of power system impedance caused by changes in power distribution equipment configuration, and variation in system management. Conventionally, Active Filters (AFs) have been utilized to cope with harmonics. In this case, however, it is necessary to readjust the control parameters according to changes in the aforementioned system characteristics. In some cases, harmonics propagation phenomena will occur. For this reason, we are requested to develop more advanced auto-tuning technologies in order to cope with various kinds of system variations.

In a mechanical system where rotary machines are used, a Permanent Magnet synchronous motor (PM motor), for example, generates torque ripples, which are regarded as periodic disturbance. These torque ripples can give rise to mechanical resonance, vibration, and noise. If torque ripples cannot be reduced by simply modifying the mechanical structure of the rotary machine, inverters may be used to cancel such a torque pulsation. In this case, however, it is necessary to perform suppression control in consideration of electrical and mechanical

transfer characteristics of inverters and mechanical systems being connected.

Against such a technological background, this paper provides explanations of our technical review on periodic disturbance suppression control technology by a generalized periodic disturbance observer with auto-learning functions on the system characteristic. In addition, as an example of application, the features of AF control against grid harmonics and torque ripple suppression control for PM motors are introduced.

2 Generalized Periodic Disturbance Observer⁽¹⁾⁽²⁾

2.1 Basic Control Configuration

Since periodic disturbance is primarily caused at a specific frequency, its frequency component is extracted to establish a suppression control system. Here, a d_nq_n rotating coordinate system (real part defined as Axis d_n , imaginary part as Axis q_n) synchronized with periodic disturbance of n -th frequency is defined. As shown in Fig. 1, I/O signals and their system transfer characteristics can then be expressed in one-dimensional complex vector. Fig. 2 shows the basic configuration of the generalized periodic disturbance observer established based on the aforementioned rotating coordinates. In this diagram, a vector notation for each signal denotes the complex vector. $G_F(s)$ is a Low Pass Filter (LPF) that functions in response to a real-and imaginary component respectively after rotating coordinate transformation. It is used for the extraction of frequency components. The real system P_n denotes the frequency transfer characteristics of the system as a whole, from input value u_n to output detection value \tilde{y}_n , including characteristics of actuator, sensor, etc. Any type of system can be generalized with simple complex vectors as indicated by Expression (1). Value P_{dn} denotes Axis d_n component of the real system in n -th frequency component and P_{qn} likewise denotes Axis q_n component.

$$P_n = P_{dn} + iP_{qn} \dots \dots \dots (1)$$

The basic operation follows up a conventional approach of disturbance observer. Based on the detection value y_n of the n -th frequency component through the LPF, Model $\hat{Q}_n (= \hat{P}_n^{-1})$ of the inverse system Q_n is used as shown in Expression (2) so that real system input \hat{u}_n is estimated as in Expression (3).

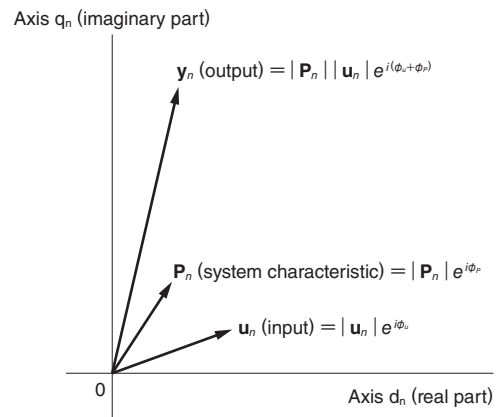


Fig. 1 Characteristic Frequency Component in Complex Vector Expression

The control system for the specific n -th order frequency component can be expressed by a primary-order complex vector in a rotating coordinate system synchronized with its frequency.

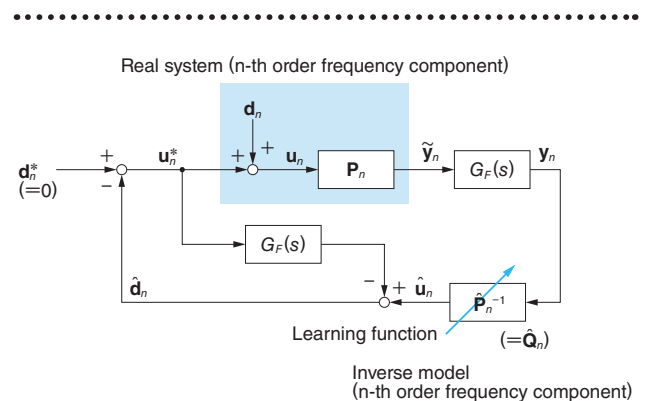


Fig. 2 Basic Configuration of the Generalized Periodic Disturbance Observer

On the rotating coordinate system synchronized with periodic disturbance, the basic configuration of the generalized periodic disturbance observer is shown expressed in a complex vector. With such a simple control configuration, periodic disturbance can be removed.

$$\hat{Q}_n = \hat{Q}_{dn} + i\hat{Q}_{qn} = \frac{1}{\hat{P}_{dn} + i\hat{P}_{qn}} \dots \dots \dots (2)$$

$$\hat{u}_n = \hat{Q}_n y_n \dots \dots \dots (3)$$

Since the real system input u_n contains the periodic disturbance d_n , Value \hat{d}_n is estimated by subtracting the current reference value u_n^* through $G_F(s)$ from \hat{u}_n of Expression (3), as indicated by Expression (4).

$$\hat{d}_n = \hat{Q}_n y_n - G_F(s) u_n^* \dots \dots \dots (4)$$

When Value \hat{d}_n of Expression (4) is subtracted from the periodic disturbance reference value d_n^* (0 in the case of suppression), it is then possible to cancel the periodic disturbance d_n .

2.2 Influence of Model Error

In actual systems, there are a variety of changes in characteristics. Value \mathbf{P}_n becomes a time-varying parameter. In this case, we have to examine the effect of Error $\hat{\mathbf{Q}}_n \neq \mathbf{Q}_n$ of the inverse model \mathbf{P}_n upon the stability of the periodic disturbance observer. Assuming that the amplitude error of the inverse model $\hat{\mathbf{Q}}_n$ is A_n ($A_n > 0$) and the phase error is ϕ_n ($-\pi < \phi_n \leq \pi$), Value $\hat{\mathbf{Q}}_n$ is defined as indicated by Expression (5). (The model is the true value when $A_n = 1$ and $\phi_n = 0$.)

$$\hat{\mathbf{Q}}_n = A_n e^{i\phi_n} \mathbf{Q}_n \dots \dots \dots (5)$$

Expression (6) below can be derived from Expression (5) by defining the periodic disturbance response from the occurrence of periodic disturbance to the acquisition of detection value. Now assume that the periodic disturbance response transfer function is $C_n(s)$, where ω_f is the cutoff frequency of primary LPF and s is a Laplace operator.

$$\frac{\mathbf{y}_n}{\mathbf{d}_n} = \frac{\omega_f s}{(s + \omega_f)(s + \omega_f A_n e^{i\phi_n})} \mathbf{P}_n = C_n(s) \mathbf{P}_n \dots (6)$$

In consideration of operation period T_s and algebraic loop avoidance to be accompanied by digital control in actual installations, Value $C_n(s)$ is z-transformed and discretized to obtain Expression (7) below.

$$C_n(z^{-1}) = \frac{z^{-1} G_F(z^{-1})(1 - z^{-1} G_F(z^{-1}))}{1 + (A_n e^{i\phi_n} - 1)z^{-1} G_F(z^{-1})} \dots \dots (7)$$

$G_F(z^{-1})$ can be regarded as a product of bilinear transformation of $G_F(s)$ and it is substituted for Expression (7) to solve a characteristic equation. Fig. 3 shows an example of numerical solution assuming that the boundary conditions of robust

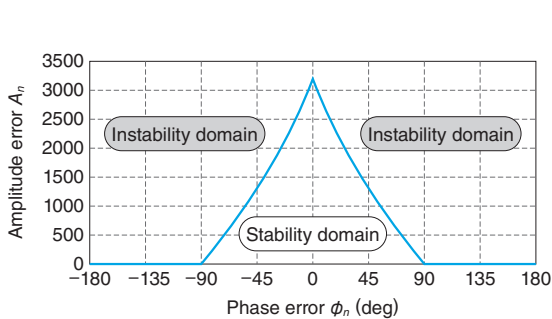
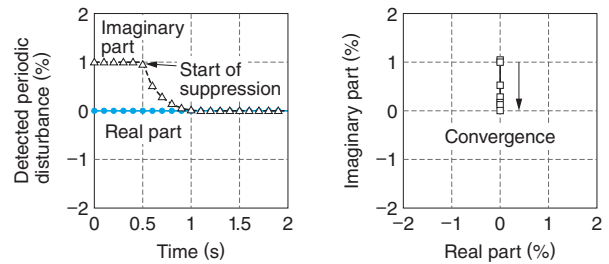


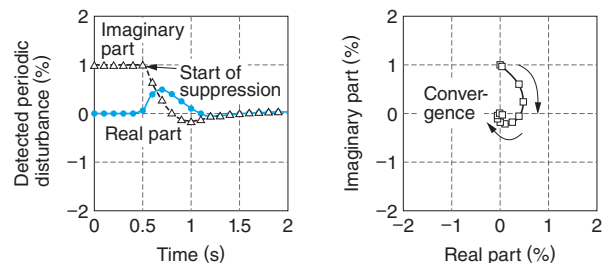
Fig. 3 Robust Stability of the Periodic Disturbance Observer

In regard to the periodic disturbance observer model, presence of stability allowance is shown where amplitude error (vertical axis) and phase error (horizontal axis) are available. There is a certain level of robust stability, but instability appears when an error becomes eminent.

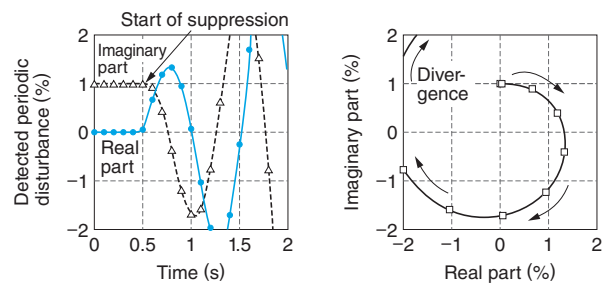
stability to model error are $T_s = 100\mu s$ and $\omega_f = 2\pi \text{ rad/s}$. As shown in this figure, the system becomes unstable when the phase error is greater than ± 90 degrees, and allowance for stability against amplitude error becomes greater as the phase error is lowered. In regard to the effect of model error of the periodic disturbance observer, Fig. 4 shows an example of an operation check based on time-serial response waveforms (left side in the figure) of the periodic disturbance detection value and loci of complex vectors (right side in the figure). As is obvious from complex vector loci, periodic disturbance converges linearly on the origin (namely periodic disturbance is zero), provided that there is no model error. Even though there is periodic disturbance, convergence is still possible if it is kept within the stability domain. Conversely, in the instability domain,



(a) Without model error ($A_n=1, \phi_n=0$)



(b) With model error (stable domain) ($A_n=1, \phi_n=\pi/3$)



(c) With model error (unstable domain) ($A_n=1, \phi_n=5\pi/9$)

Fig. 4 Relationship between Model Error and Vector Locus

In regard to influence by model error of the periodic disturbance observer, time-related response waveform (left) and the locus of complex vector (right) are shown. According to the amount of model error, the locus changes at the time of convergence on the origin and it diverges when the amount of error is large.

periodic disturbance diverges, drawing a circle. In this case, periodic disturbance cannot be suppressed.

According to the descriptions above, the periodic disturbance observer is a control system having a robust property against model error. Its control, however, can be unstable if there is a large model error or any variation in characteristics of the operating system. In this connection, the auto-learning function for the detection and correction of model error will be explained in the next paragraph.

2.3 Auto-Learning Function of Model Error

As shown in Fig. 4, there is a specific relationship between model error and complex vector locus. Paying attention to the geometrical information of this locus, we propose an approach for the detection and correction of the model error.

Initially, we determine the detection value \tilde{y}_n of the n -th order periodic disturbance before LPF and the average value \bar{y}_n with the learning control period T_L . Then, in order to examine the response at time t on the complex plane of the average value \bar{y}_n for n -th order periodic disturbance detection, we define Amplitude R_n and Phase Ψ_n on the polar coordinates as indicated by Expression (8). As suggested by Expressions (9) and (10) and Fig. 5, we define the origin-direction vector \mathbf{R}_n , periodic disturbance movement vector \mathbf{L}_n , and angle ϕ_n between \mathbf{R}_n and \mathbf{L}_n , and then assume that the amount of periodic disturbance vector movement at micro-time ΔT is ΔL_n , the amount of change in amplitude is ΔR_n , and the amount of change in phase is $\Delta \Psi_n$. As a result, Expressions (11) and (12) hold according to the geometrical relationship on the polar coordinates.

$$\bar{y}_n = R_n(t) e^{i\Psi_n(t)} \dots \dots \dots (8)$$

$$\mathbf{R}_n = -\bar{y}_n(t - \Delta T) \dots \dots \dots (9)$$

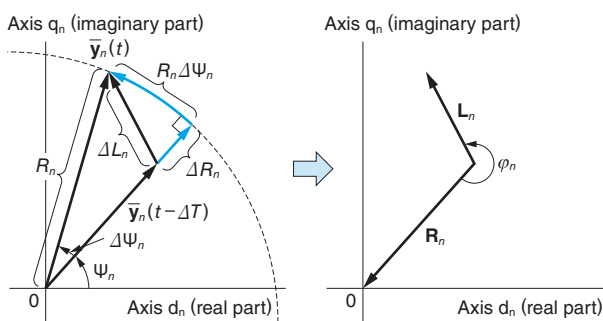


Fig. 5 Various Definitions for Complex Vector Locus

Definition of the complex vector locus is shown in regard to geometric information.

$$\mathbf{L}_n = \bar{y}_n(t) - \bar{y}_n(t - \Delta T) \dots \dots \dots (10)$$

$$\Delta L_n(t) = \sqrt{\Delta R_n(t)^2 + R_n(t)^2 \Delta \Psi_n(t)^2} \dots \dots \dots (11)$$

$$\begin{aligned} \phi_n(t) &= \tan^{-1} \left(\frac{|\mathbf{R}_n \times \mathbf{L}_n|}{\mathbf{R}_n \cdot \mathbf{L}_n} \right) \\ &= \tan^{-1} \left(\frac{-R_n(t) \Delta \Psi_n(t)}{-\Delta R_n(t)} \right) \dots \dots \dots (12) \end{aligned}$$

As a result of the inverse Laplace transformation of response to periodic disturbance up to \bar{y}_n in the case of application of a step disturbance input to \mathbf{d}_n as shown in Fig. 2, a time response equation of Expression (13) is obtainable. In this case, however, operation dead time is: $\Delta T = T_L$.

$$\begin{aligned} \bar{y}_n(t) &= \mathcal{L}^{-1} \left[\frac{s}{s + \omega_f A_n e^{i\phi_n}} e^{-sT_L} \cdot \frac{1}{s} \right] \mathbf{P}_n \\ &= \mathbf{P}_n e^{-A_n \omega_f \cos \phi_n \cdot (t - T_L)} e^{-iA_n \omega_f \sin \phi_n \cdot (t - T_L)} \dots \dots \dots (13) \end{aligned}$$

When Expression (13) is compared with Expression (8), Values R_n and Ψ_n on the polar coordinates can be expressed in Expressions (14) and (15) below.

$$R_n(t) = \mathbf{P}_n e^{-A_n \omega_f \cos \phi_n \cdot (t - T_L)} \dots \dots \dots (14)$$

$$\Psi_n(t) = -A_n \omega_f \sin \phi_n \cdot (t - T_L) \dots \dots \dots (15)$$

When Expressions (14) and (15) and differential equations (16) and (17) at the learning control period T_L are substituted for Expressions (11) and (12), Expressions (18) and (19) can be obtained.

$$\begin{aligned} \Delta R_n(t) &= R_n(t) - R_n(t - T_L) \\ &\simeq -\mathbf{P}_n A_n \omega_f \cos \phi_n e^{-A_n \omega_f \cos \phi_n \cdot t} T_L \dots \dots (16) \end{aligned}$$

$$\begin{aligned} \Delta \Psi_n(t) &= \Psi_n(t) - \Psi_n(t - T_L) \\ &= -A_n \omega_f \sin \phi_n T_L \dots \dots \dots (17) \end{aligned}$$

$$\Delta L_n(t) \simeq \mathbf{P}_n A_n \omega_f e^{-A_n \omega_f \cos \phi_n \cdot t} T_L \dots \dots \dots (18)$$

$$\phi_n(t) \simeq \phi_n \dots \dots \dots (19)$$

When Expression (18) is divided by Expression (14) and then rearranged in terms of amplitude error A_n , a relationship of Expression (20) can be obtained.

$$A_n \simeq \frac{\Delta L_n(t)}{\omega_f R_n(t) T_L} \dots \dots \dots (20)$$

Judging from the result of analysis described above, the following relationship holds between the periodic disturbance vector locus on the complex plane and model error:

- (1) Phase error ϕ_n is equal to Angle ϕ_n between the periodic disturbance vector locus on the complex plane and the direction to the origin.

(2) Amplitude error A_n can be detected from the ratio of the amount of periodic disturbance vector movement ΔL_n versus Distance R_n from the origin.

For the detection of a model error in an actual case, however, it is necessary to bear in mind some significant facts such as the effect of characteristic variation in periodic disturbance other than step disturbance and measurement-borne noise during the execution of detection through arbitrary filter treatment. Model error is estimated with the use of Expressions (19) and (20) obtained from detection. In the case of deterioration of robust control performance in the periodic disturbance observer, the model is sequentially corrected based on the estimated value. In this manner, control can be automatically stabilized even in the unstable domain as stated in Section 2.2 above. In addition, it is possible to improve control performance like a quick response reaction in the stable domain.

Fig. 6 shows an example of a comparison between with or without an auto-learning function at $A_n = 0.5$ and $\phi_n = 5\pi/9$ (unstable domain). For a model without a learning function, divergence occurs immediately. In the case of a model with a learning function, however, phase error of the model

is first detected and corrected so that the error is correctly suppressed in the direction of convergence. Subsequently, amplitude error is corrected for the improvement of converging speed.

The features of our proposed method are summarized below.

- (1) Since the system transfer functions of periodic disturbance are generalized with simple complex vectors, our method is applicable even to a complicated control object.
- (2) When multiple periodic disturbance observers are installed in parallel to each other, multiple frequency components can be managed.
- (3) Even though variations in system characteristics and initial values of parameters are unknown, it is possible to stabilize and improve the control performance while operation for suppression is continued with the use of the auto-learning function.

3 Application to Power AF

In order to investigate potential applications of our generalized periodic disturbance observers provided with auto-learning functions introduced in the forgoing sections, we have examined the AF used in the power distribution system. Fig. 7 shows an empirical circuit configuration of the AF. The voltage source inverter functioning as an AF is connected in parallel to the interconnection point. Two types of

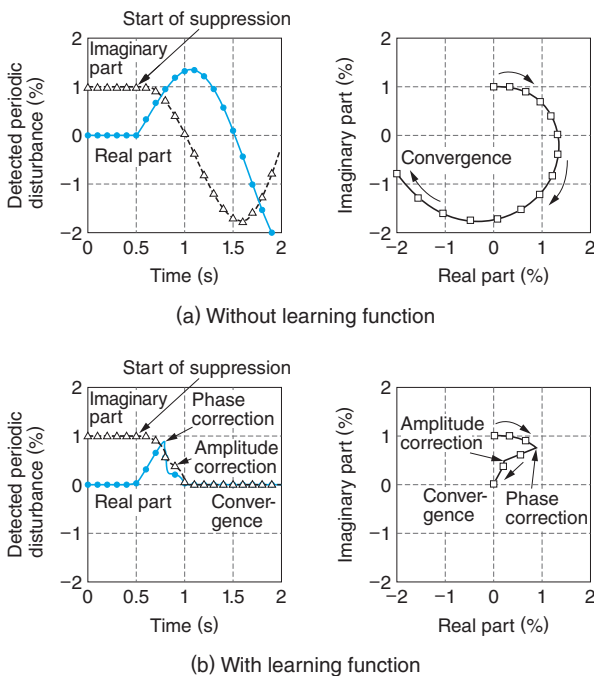


Fig. 6 Effect of the Auto-Learning Function for the Model

The effect of the auto-learning function is verified, for which the model error of the periodic disturbance observer is compensated. Time-based response waveform (left) and complex vector locus (right) are shown. Periodic disturbance is diverged without learning function, while it is converged on the origin when the learning function is used, and phase and amplitude errors are adjusted.

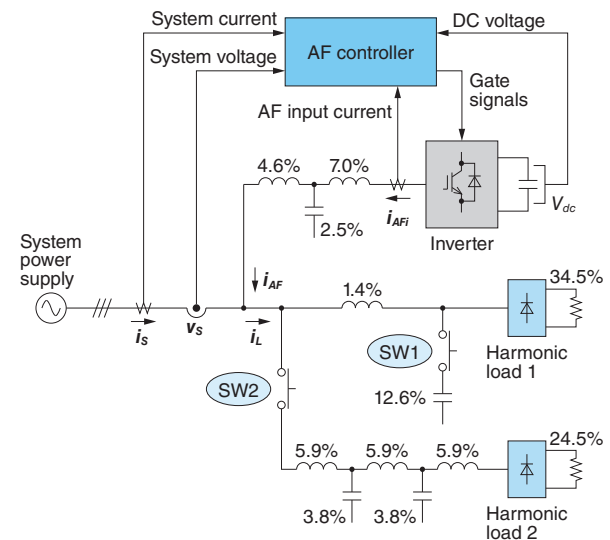


Fig. 7 Empirical Circuit Configuration of AF

This is empirical equipment intended to suppress harmonics in the power distribution system with the use of AF. In this case, the source current detection system is applied in order to suppress harmonics by feeding back the system current. Using the switches SW1 and SW2, impedance variations are simulated during suppression.

diode rectifier loads being the source of harmonics are also connected. The Switch SW1 is installed on the assumption that a phase-advancing capacitor bank is turned on in the middle of suppression operation. It is intended to modify the impedance characteristics of the harmonics load 1. Switch SW2 connected with the harmonics load 2 is used to simulate impedance characteristic changes in power distribution system and an increase in current carried in the harmonics load.

The control system of the AF is classified according to the positions for the detection of harmonics, i.e. load current detection system, source current detection system, and voltage detection system. The voltage detection system, in principle, assures a greater allowance in stability than that of the current detection system and is effective in terms of harmonics propagation phenomena and damping property against system resonance. It is, however, difficult to suppress a system's current harmonics with high accuracy.

The source current detection system can also assure accurate compensation through direct detection of harmonic current that flows into the system. This system, however, is liable to be influenced by impedance characteristic changes and control can become unstable. This paper describes our approach where the source current detection system is adopted to maintain harmonics suppression accuracy, the auto-learning function is used to raise control stability, and difficulties of both are compensated for accordingly. Our system is applicable on-line to unknown variations in impedances of power distribution systems that have been considered difficult to cope with.

At the AF control block, the basic vector control of the inverter current synchronized with system voltage phase and control of DC voltage are carried out. In this state, harmonics suppression control of system current is i_s carried out with the use of the generalized periodic disturbance observer that has an auto-learning function explained elsewhere in forgoing paragraphs.

Fig. 8 shows an example of an experimental result concerned with the power AF. Harmonics of 5th, 7th, 11th, and 13th order are the object of suppression. The upper diagram shows the system currents and also their real and imaginary components at each order. The lower diagram is an enlarged one where Sections A, B, and C in the upper diagram are shown. They are the waveforms of load current

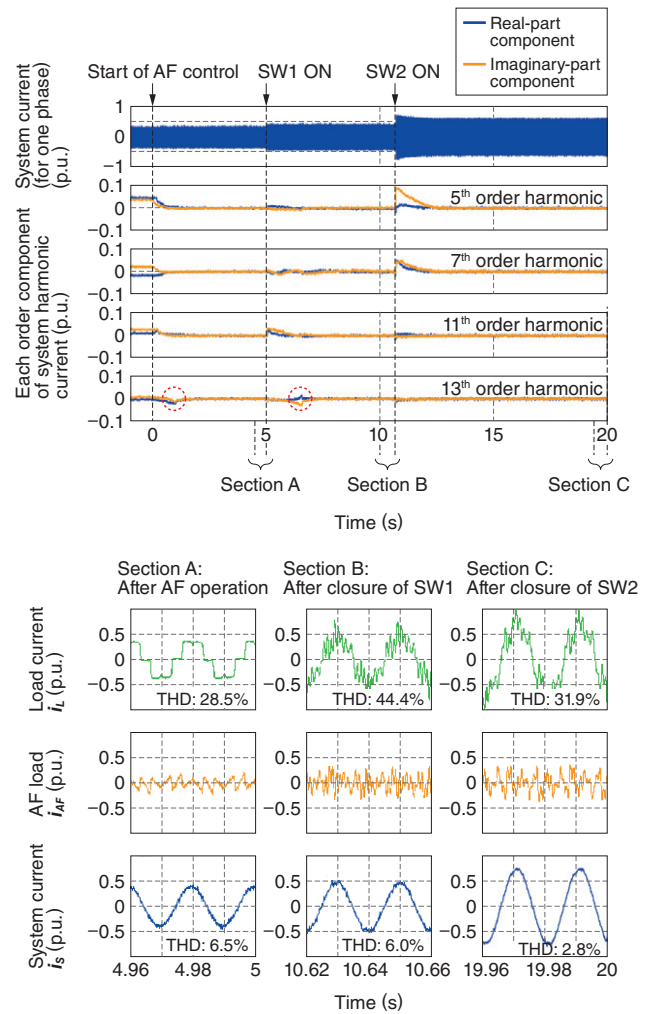


Fig. 8 Result of Experiment on AF

AF control is started under the condition that the initial value of the model is incorrect, and switches SW1 and SW2 are turned on so that steep variation in power distribution system impedance and increase in harmonic currents are actually created. Stable and preferable suppression performance, however, is obtained by virtue of auto-learning function.

i_L , AF compensation current i_{AF} , and system current i_s , respectively. Before the start of AF operation, the system is in such a condition that waveforms of load current including a distortion component are about to flow into the system directly. At Time 0, suppression control is started from a state where model's initial value of the periodic disturbance observer is still incorrect. After the start, components of 5th, 7th, and 11th order harmonics can be suppressed because the model error is kept within the robust stability domain of the periodic disturbance observer. As indicated by dotted circles, the model error conversely remains to stay in the instability domain and components of the 13th order harmonics once go on in the direction of divergence. Due to the effect of auto-learning function, however, the model error is

adjusted and these components likewise go on in the direction of convergence and suppression is finally completed. Successively, SW1 for the connection of a phase advancing capacitor bank is turned on in order to simulate variations in impedance characteristics during operation of suppression. Also in this case, the 13th order harmonics go on again in the direction of divergence due to the effect of model error. Similarly, when SW2 is turned on to increase the harmonic current rapidly, suppression control can be continued without any problem. Judging from waveforms of the system current, it can be realized that harmonic distortion is removed and the resultant load current appears in a sinusoidal waveform. Total Harmonic Distortion (THD) is also reduced and the obtained result appears preferable.

As described above, application of our proposed control system is expected to result in the following effects:

- (1) For a system where impedance characteristics are unknown, it is unnecessary to perform any system identification in advance nor any parameter adjustments for suppression control.
- (2) Even though any impedance characteristic should change in the middle of suppression operation, system instability cannot be caused and prevention of harmonics propagation phenomena and the improvement of suppression performance can be automatically accomplished.

4 Application to Motor Torque Ripple Suppression⁽¹⁾⁻⁽³⁾

For another example of application of the periodic disturbance observer, Fig. 9 shows an empirical configuration of torque ripple suppression control for PM motors. Inverters are used to perform a speed controlled operation by generalized vector control and the coupling shaft between the PM motor and the load is equipped with a torque meter. Since torque ripples are considered to be a kind of periodic disturbance generated in synchronization with rotating phase θ , frequency components of n -th torque ripples T_{dn} and T_{qn} are arbitrarily extracted from the detected torque value T_{det} so that suppression control is performed with the use of the aforementioned periodic disturbance observer. In this case, however, a frequency of torque ripples also changes during speed-controlled operation. In the case of a model for the periodic disturbance observ-

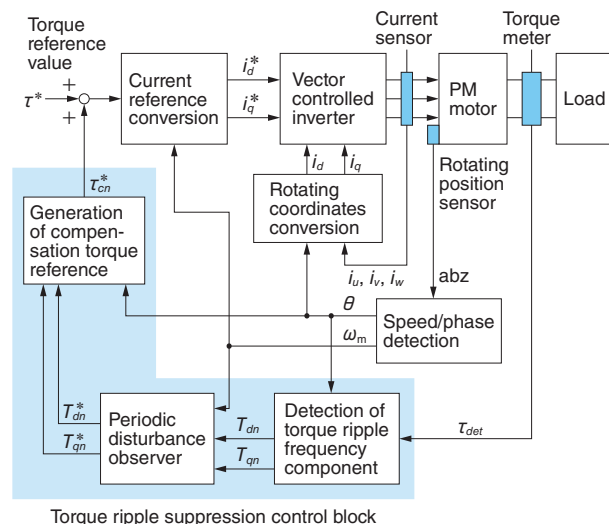
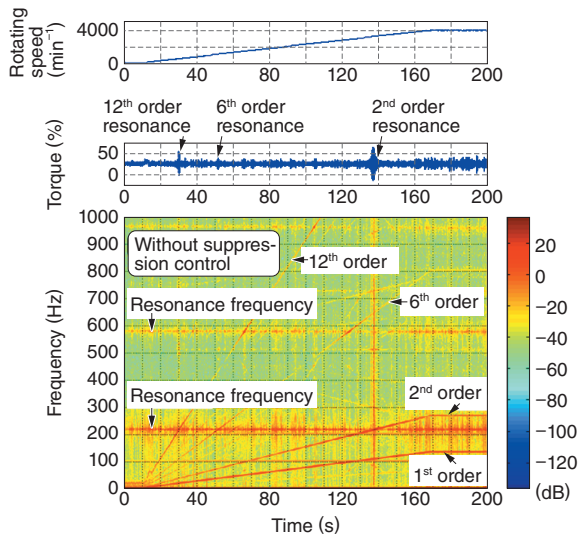


Fig. 9 Empirical Configuration of Torque Ripple Suppression Control

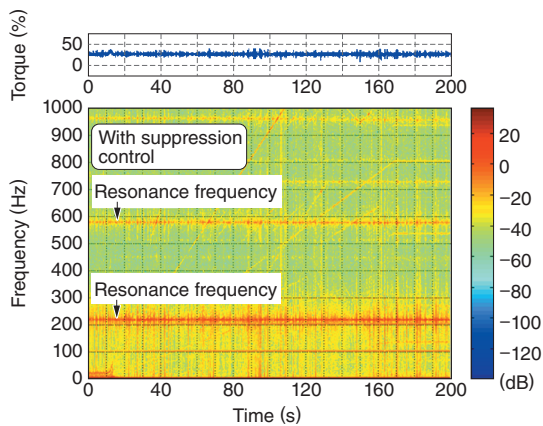
A system configuration is shown, where torque ripple frequency component synchronized with motor rotating speed is detected and it is controlled with the periodic disturbance observer.

er, its characteristics have to be therefore modified into system transfer characteristics according to the specific frequency. For this reason, we have devised to set up the tabulation of real and imaginary components of frequency transfer characteristics in advance at the time of system identification. For example, for the tabulation of frequency transfer characteristics in a range of 1~1000Hz at the intervals of 1Hz, the table can be established with the use of 1000 complex vectors. Using the number of revolution ω_m , a complex vector corresponding to the torque ripple frequency is extracted from the table and applied as a model for the periodic disturbance observer. In this method, torque ripples can be suppressed even in the middle of speed-controlled operation by sequentially updating the model.

Fig.10 shows the result of experiments to investigate the torque ripples in the middle of a speed-controlled operation using the spectrograms (short-time Fourier analysis: time on the horizontal axis, frequency on the vertical axis, and the spectrum indicating the intensity of frequency component). The spectrum (in the vicinity of 210Hz and 590Hz) remained unchanged even with a change in time as a component of resonance frequency in the mechanical system. The spectrum with a frequency, changing with an increase in rotating speed, corresponds to torque ripples. Judging from the result of operation without suppression control, conspicuous effects appear with 1st, 2nd, 6th, and 12th order com-



(a) Without suppression control



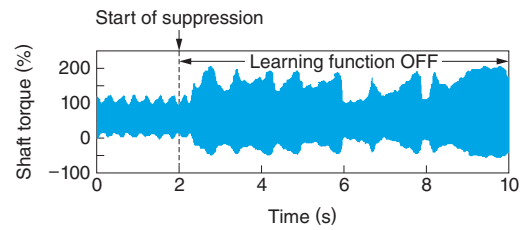
(b) With suppression control

Fig. 10 Result of Speed Control Experiments on Torque Ripple Suppression Control

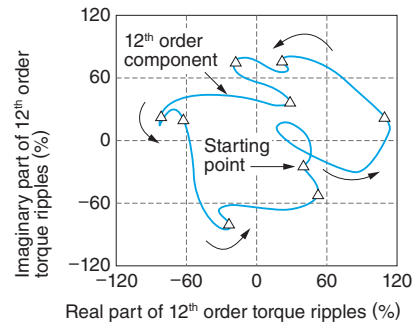
The result of spectrogram verification is shown, performed to verify the effect of suppression in the middle of speed-controlled operation. The spectrum intensity of middle ripples is reduced by the effect of suppression control and large torque resonance is also suppressed.

ponents. In particular, a large torque resonance seems to occur at a crossing point with resonance frequency. In the case of operation with suppression control, spectra of components at the respective orders are sharply reduced and this is a good result verifying that there is no occurrence of any remarkable resonance. We have made many of other verification experiments in regard to, for example, a system where no torque meter is used or a system of feed-forward approach with accumulated data such as results of measurements of transient and other phenomena.

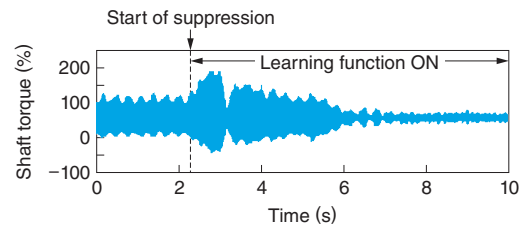
As described previously, the applied model is sequentially updated during speed-controlled operation. It is, therefore, not very easy to perform model-based correction by using auto-learning



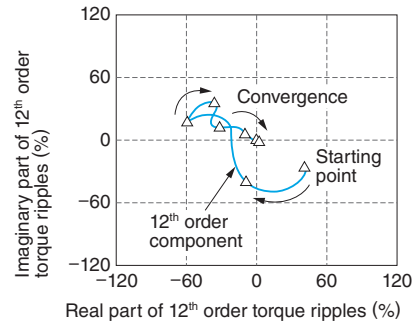
Learning function OFF



(a) Without learning function



Learning function ON



(b) With learning function

Fig. 11 Empirical Result of Auto-Learning Function for Torque Ripple Suppression Control

When the motor is in a state of steady operation (constant torque, constant rotating speed), the auto-learning function is used to correct the model error.

function. Under specific conditions, there may be a case when secular variations can occur in characteristics of the motor driving system. As such, we make it a rule to use the auto-learning function of the model limited only to the cases when the motor is in steady-state operation (without changes in rotating speed and torque). Fig. 11 shows the result of experiments where the auto-learning function is applied. At the rotating speed of resonance with 12th order torque ripple component, experiments are

started from a state where the model's initial value is incorrect. When no learning function is used, control begins to diverge upon the start of suppression and the locus continues to move in unstable mode while the torque reference value keeps on saturating. With the learning function, once control once on diverging, but immediately afterwards, the model is quickly updated and suppression of torque ripples is successfully accomplished.

Judging from the aforementioned, torque ripple suppression for the PM motor by our proposed control system is expected to offer the following effects:

- (1) Torque ripples can be suppressed even in the middle of speed-controlled operation insofar as the system's frequency transfer characteristics are tabulated in advance.
- (2) Even though the initial values of parameters in the motor or a mechanical system are unknown, the model is automatically updated and torque ripples can be suppressed, provided that they are in the state of steady-state operation.

5 Postscript

This paper introduced the generalized periodic disturbance observer system that has an auto-learning function developed as an approach for periodic disturbance suppression technologies. As an example of application, features of the AF for power system harmonics and torque ripple suppression for PM motors have been examined in this paper. The usefulness of this system is theoretically verified

based on the result of experiments. Although this system is arranged into a simple control configuration, it has exhibited a capability of automatic suppression of periodic disturbance for any system where complicated characteristics and variations are involved. Our technologies are those of environmental coordination to solve problems of systematic products such as vibration, noise, and resonance. These technologies are also related to the attainment of easy maintenance by automated adjustments and the improvement of control quality. Our control technologies are generalized and applicable to horizontal development toward other systems. Going forward, we intend to continue developing these applications.

- All product and company names mentioned in this paper are the trademarks and/or service marks of their respective owners.

《References》

- (1) Y. Tadano, T. Akiyama, M. Nomura, M. Ishida: "Periodic Learning Suppression Control of Torque Ripple Utilizing System Identification for Permanent Magnet Synchronous Motors," IEEE International Power Electronics Conference (IPEC-Sapporo 2010), pp.1363-1370, 2010.6
- (2) Y. Tadano, T. Akiyama, M. Nomura, M. Ishida: "Torque Ripple Suppression Control Based on the Periodic Disturbance Observer with a Complex Vector Representation for Permanent Magnet Synchronous Motors," IEEJ Transactions on Industry Applications, Vol.132, No.1, pp.84-93, 2012.1 (in Japanese)
- (3) T. Yamaguchi, Y. Tadano, N. Hoshi: "Torque Ripple Suppression Control by Periodic Disturbance Observer with Model Error Correction," IEEJ Transactions on Industry Applications Vol.134, No.2, pp.185-192, 2014.2 (in Japanese)